Experimental and Numerical Evaluation of Analytical Volume Balance Model for Soil Water Dynamics under Drip Irrigation

Khumoetsile Mmolawa and Dani Or*

ABSTRACT

The interpretation and subsequent modeling of soil water dynamics in presence of active plant uptake remains a challenge. Despite many simplifying assumptions in their development, analytical models offer simple and easy means for prediction of soil water dynamics that could be readily generalized for development of design and management guidelines. A local volume balance analytical model for predicting soil water dynamics was recently developed and successfully tested with a few point measurements. However the validity of various simplifying assumptions and rigorous evaluation of the model across an entire root zone with spatially variable water distribution was not tested. The objective of this study was to evaluate the analytical model relative to measurements and to a widely used numerical model (Hydrus-2D [H2D]). Both models were first fitted to measured data at selected locations to estimate hydraulic parameters for subsequent modeling of the entire flow domain. Water content dynamics by the analytical model was in good agreement with the H2D model simulations in the absence of plants. With active plant uptake, the analytical model overestimates root water uptake at some locations when compared with H2D. This was attributed to the lack of consideration of water stress effects due to changing soil-water status on uptake intensity in the analytical model. The analytical model was also sensitive to the choice of linearizing hydraulic parameters that in turn are dependent on the range of soil water content in the simulation domain.

As water infiltrates into the soil, water content changes both spatially and temporally according to soil type, boundary, and initial conditions. Root uptake patterns of water and solutes are highly dynamic within the soil profile because root distribution within the soil profile, water content and availability, and aeration status are in a constant state of change (Mmolawa and Or, 2000a,b).

Modeling water and solute dynamics often requires knowledge of plant root distribution and activity. The common approach for modeling soil water dynamics is to relate root length or mass distribution to water uptake patterns. According to Molz (1971), the relationship between root distribution and root uptake of water is complicated by the fact that the volume or mass of roots in a given location does not necessarily reflect their ability to absorb water. Parameters for casting root water uptake models are crop specific, and vary among growing conditions. Moreover, the disparity between root distribution and water uptake patterns destine models that rely solely on root distribution for modeling water dynamics to failure (Clothier et al., 1990; Coelho and Or, 1999). Despite difficulties in formulating satisfactory root water uptake models, such models are essential for delineation of soil water dynamics in cropped root zones. At the macroscopic scale, the root system is usually represented by a volumetric sink term, which is added to the Richards' equation (see below *Water Flow from Point Sources*) governing water flow (Feddes et al., 1974; Hillel et al., 1976a). The macroscopic approach ignores details of flow patterns toward individual roots and thus avoids the geometric complications involved in considering distribution of fluxes and potential gradients to individual roots. However, the main disadvantage of the macroscopic approach is that it is based on gross spatial averaging of the matric and osmotic potentials, and therefore disregards the increase in suction and salt concentration in the close vicinity of the absorbing roots (Hillel et al., 1976a). Although the lumped macroscopic sink term approach is more convenient for modeling root water uptake, it often fails to improve understanding of water uptake by plant roots as offered by a microscopic approach (Aura 1996). The microscopic approach represents a single root by a cylinder equivalent to a line source of uniform thickness and infinite length having uniform water absorbing properties (Feddes et al., 1974; Aura, 1996; Hillel et al., 1976b; Heinen, 1997).

Coelho and Or (1996a) developed an analytical model for soil water dynamics including spatially distributed plant water uptake using a local volume balance approach. It has since been tested for a range of point measurements by Coelho and Or (1996 a,b), and by Mmolawa and Or (2000a,b). However, a rigorous evaluation of the approximations for deriving this model has not been attempted over an entire cross-section of drip irrigated crop root zone. For lack of better tools, we propose to test the approximations made by the analytical model with the detailed numerical model H2D (Simunek et al., 1999). These two models will be evaluated in both the absence and presence of plant water uptake. The linearized hydraulic parameters essential for application of the analytical model (see below *Water Flow from Point Sources*) were estimated and tested for selected points but their applicability for the entire cross-section was not evaluated. This is important because the linearization parameters vary with water content. Thus, it is expected that for simulations using a certain set of parameters the analytical model performance is likely to deteriorate due to the natural gradient of water content around an emitter which spans a wider range of conditions than used for parameter estimation. Finally, because the analytical model uses superpositioning (in

Dep. of Biological and Irrigation Engineering and Dep. of Plants, Soils and Biometeorology, Utah State Univ., Logan, UT 84322-4820. D. Or now at Dep. of Civil and Environmental Engineering, Univ. of Connecticut. Received 10 Nov. 2000. *Corresponding author (dani@engr.uconn.edu).

Published in Soil Sci. Soc. Am. J. 67:1657–1671 (2003).

677 S. Segoe Rd., Madison, WI 53711 USA

Abbreviations: H2D, Hydrus-2D model.

space and time) of water flow and plant uptake (Or and Coelho, 1996), we expect soil water dynamics at a location to be influenced by partial flux interception by plant roots. Hence the validity of spatial superposition schemes that assume the flux is unaltered must be tested. In contrast, the H2D model does not rely on a linearization procedure for soil water flow predictions but rather numerically solves the Richards' water flow equation combined with a distributed plant uptake sink identical to the one used for the analytical model to simulate soil water dynamics.

The main objective of this study was thus to test the simplifying assumptions made in deriving the analytical model by evaluating the model performance relative to field measurements and in comparison with detailed numerical simulations by the H2D model. The specific objectives were to (i) test the performance of the analytical model using constant linearizing hydraulic parameters at individual locations and a representative set of values for the entire cross-section, (ii) test the validity of spatial superpositioning of water flow and plant uptake (as two independent processes) at different locations and the resulting prediction of water content dynamics in the presence of plants.

Generally the evaluation will entail comparison of results from the two models at arbitrarily chosen locations in the simulated domain, as well as for the entire root zone cross-section. Simulations performed with the models were compared with measured data. The first part of this study's theoretical section provides an overview on water flow from point sources, followed by details of the analytical solution with an outline of the local volume approach used for incorporating root water uptake. The second part of the theoretical section is devoted to a brief review of the H2D model. In the *Materials and Methods* section we briefly outline the conducted experiments and explain how the measured cross-sectional two-dimensional water uptake (see Fig. 1a.) is attributed to a smaller surface area sitting above the uptake cross-section. The methods section also explains the transformation of the two-dimensional cross-sectional uptake to a full three-dimensional radial coordinate system used by the H2D model.

THEORY

Water Flow from Point Sources

Multidimensional infiltration and subsequent distribution of water from point sources in soil is modeled by the Richards' equation that combines Darcy's law with conservation of mass as

$$\frac{\partial \theta}{\partial t} = \nabla\,(K \nabla H) \qquad [1]$$

where θ is the volumetric water content ($m^3\ m^{-3}$), K is the hydraulic conductivity function ($m\ s^{-1}$), H is the total head (m) (expressed as the sum of matric head, h, and gravitational head, z), ∇ is the spatial gradient operator.

Analytical solutions for Eq. [1] can be obtained by a linearization procedure (Philip, 1971) that uses the matric flux transformation variable (ϕ) proposed by Gardner (1958) as

$$\phi = \int_{-\infty}^{h} K(h)\mathrm{d}h = \frac{K(h)}{\alpha} \qquad [2]$$

where h (m) is the matric head, α (m^{-1}) represents the rate of reduction in hydraulic conductivity with h, $K(h)$($m\ s^{-1}$) is the unsaturated hydraulic conductivity defined as

$$K(h) = K_s \exp(\alpha h) \qquad [3]$$

where K_s ($m\ s^{-1}$) is the saturated hydraulic conductivity.

Analytical Solution for Transient Flow from a Point Source

Warrick (1974) used Eq. [2] and [3] and the additional assumption that the slope of the $K(\theta)$ versus θ relationship, $k = \mathrm{d}K/\mathrm{d}\theta$, is assumed to be constant to linearize Eq. [1] into

$$\frac{\partial \phi}{\partial t} = \frac{k}{\alpha}\nabla^2 \phi - k\frac{\partial \phi}{\partial z} \qquad [4]$$

Equation [4] was solved analytically using the dimensionless variables $R = \alpha r/2$, $Z = \alpha z/2$, $T = \alpha k t/4$, and $\rho = (R^2 + Z^2)^{0.5}$, where r and z are cylindrical coordinates, t is time, and the dimensionless matric flux potential (Φ) is

$$\Phi = \frac{\alpha q \phi}{8\pi} \qquad [5]$$

where q is the point source strength or discharge ($m^3\ s^{-1}$), with the initial condition (i.e., $t = 0$)

$$\phi(r,z,0) = 0 \qquad [6]$$

and the boundary condition

$$\frac{-\partial \phi}{\partial z} + \alpha\phi = 0 \qquad [7]$$

for $z = 0$, $r \neq 0$.

The dimensionless analytical solution for a point source buried in an infinite medium is given as (Warrick, 1974)

$$\Phi_{pB}(R,Z,T) = \frac{\exp z}{2\rho}\left[\exp \rho\ \mathrm{erfc}\left(\frac{\rho}{2\sqrt{T}} + \sqrt{T}\right) + \exp(-\rho)\ \mathrm{erfc}\left(\frac{\rho}{2\sqrt{T}} - \sqrt{T}\right)\right] \qquad [8]$$

where R, Z, T, and ρ are dimensionless variables as defined in Eq. [4], erfc is the complimentary error function (available in most computer spreadsheets) given as (Spiegel and Liu, 1999),

$$\mathrm{erfc}(x) = 1 - \mathrm{erf}(x) = \frac{2}{\sqrt{\pi}}\int_x^{\infty} \exp - u^2\,\mathrm{d}u$$

For temporal variations in source strength, as is the case of drip irrigation cycles, the matric flux potential, ϕ, is obtained by superposition and use of Eq. [5] (Warrick, 1974; Coelho and Or, 1996a), and is given by

$$\phi(R,Z,T) = \frac{\alpha}{8\pi}\sum_{i=0}^{n}(qi - q_{i-1})\Phi(R,Z,T - T_i) \qquad [9]$$

for $q_{-1} = 0$, $T_0 = 0$, and $T > T_i$

Matric head values can then be obtained from the transformations (Eq.[2] and [3])

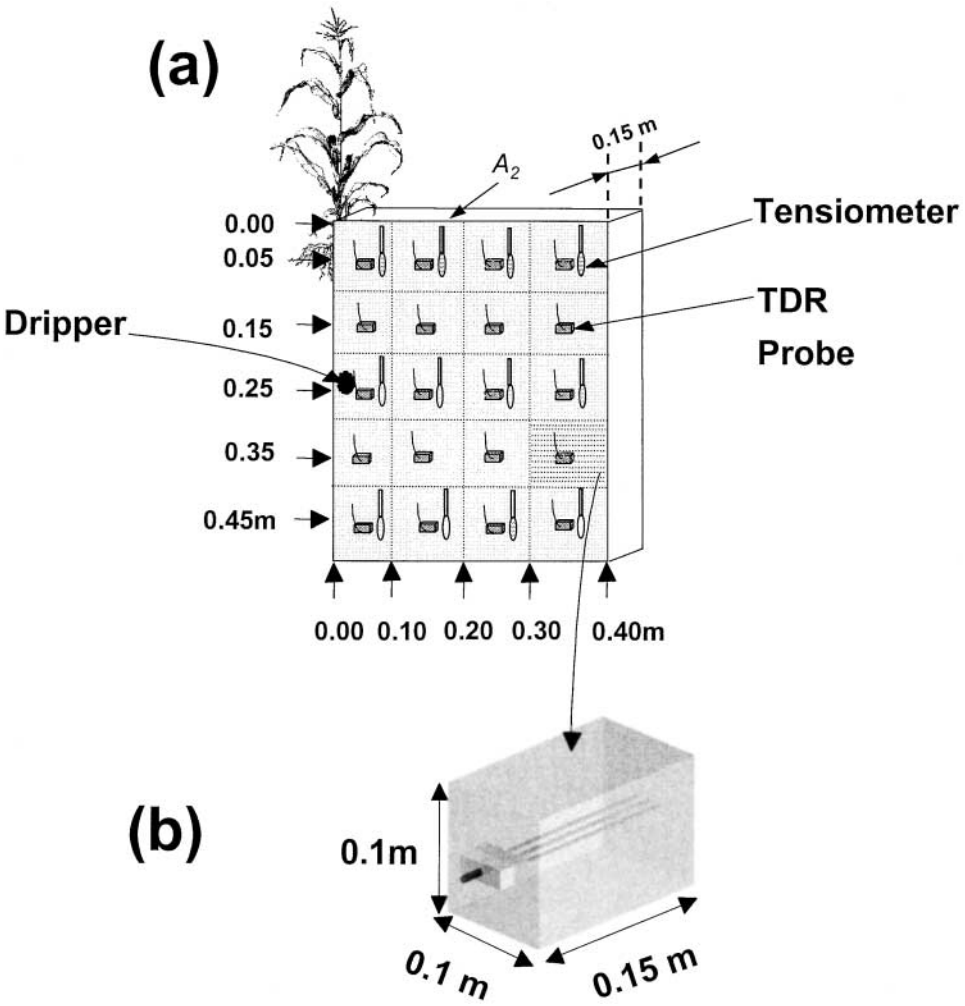

Fig. 1. (a) Cross-sectional view of time domain reflectometry (TDR) monitoring grid for soil water status under cropped and non-cropped situations. The surface area (A_2) attributed to this cross-sectional uptake is 0.15 by 0.40 m = 0.06 m^2. (b) Control soil volume for local volume balance calculation.

$$h(r,z,t) = \frac{1}{\alpha}\ln\left(\frac{\alpha\phi(r,z,t)}{K_s}\right) \qquad [10]$$

The corresponding transient soil water content values [$\theta_{flow}(r,z,t)$] are obtained via soil water retention models (van Genuchten, 1980: Russo, 1988). The van Genuchten (1980) model is given as:

$$\frac{(\theta_{flow} - \theta_r)}{(\theta_s - \theta_r)} = \left[\frac{1}{1 + (\alpha_{VG}h)^n}\right]^m \qquad [11]$$

where θ_r and θ_s are the residual and saturated water contents respectively, n is a dimensionless parameter related to the shape of the $\theta(h)$ curve, $m = 1 - 1/n$, and α_{vG} (m^{-1}) is a constant related to the soil sorptive properties. It has the same dimensions as α in Gardner's (1958) (Eq. [3]). Throughout this paper this notation for α_{VG} and α is followed hereafter. The retention model of Russo (1988) is given as:

$$\frac{(\theta_{flow} - \theta_r)}{(\theta_s - \theta_r)} = \left[\exp(0.5\,\alpha h)\,(1 - 0.5\alpha h)\right]^{\frac{2}{\mu+2}} \qquad [12]$$

where μ is a pore connectivity parameter whose value is taken to be 0.5 for our subsequent applications. The Russo (1988) model is more appropriate for the linearized equations because it is based on the same parameter α, used in the calculation of ϕ (Coelho and Or, 1996a), and was derived by using the exponential hydraulic conductivity function (Eq. [3]).

Local Water Balance Approach for Soil Water Dynamics

In their soil water dynamics study, Coelho and Or (1996a) proposed a model for estimating root uptake of water. They made an assumption whereby transient soil water dynamics at any position in the cross-section (r,z) result only from interactions between root extraction and water flow emanating from the point source (dripper) predicted by Eq. [11] or [12]. Moreover, the duration of an irrigation event is shorter than the uptake time scale, hence these processes of water flow and plant uptake can be separated and treated by linear superpositioning in time for a fixed point in space. Other likely influences from soil evaporation and deep percolation were considered negligible. Thus water content prediction at any given location (r,z) is due to the analytical transient flow solution (Eq. [11] or [12]), and changes in water content due to plant uptake within the same volume element (r,z).

The resultant water content at a given location(r,z) can be obtained in three steps, the first being to convert Eq. [10] to $\theta(r,z,t)$ through Eq. [11] or [12], that is., substituting h from Eq. [10] into either Eq. [11] or [12]. In the second step we calculate changes in water content ($\Delta\theta$) attributed to cumulative plant water uptake since time t_0 as

$$\Delta\theta_{uptake}(r,z,t - t_0) = \int_{t_0}^{t} u^*(r,z)\mathrm{d}t \qquad [13]$$

where $u^*(r,z)$ is the actual water uptake function at a given location (r,z), given by the product of the plant transpiration rate (T) and the uptake intensity function $[u(r,z)]$, [i.e., $u^*(r,z) = u(r,z) \times T$], the dimensions of the water uptake function are $L\,T^{-2}$. The function $u(r,z)$ $(m^3\,m^{-3}\,d^{-1})$ represents the two-dimensional uptake intensity distribution scaled by the total uptake intensity for a given cross-section (see Fig. 1). Spatial distribution of uptake intensity $u(r,z)$ varies with different drip-crop row configurations (see Fig. 1 in Or and Coelho, 1996), specifically, for a buried dripper in a crop row, $u(r,z)$ is parameterized as a bivariate normal distribution function (Or and Coelho, 1996a),

$$u(r,z) = \frac{\beta}{2\pi s_s s_z}\exp\left\{-0.5\left[\frac{(r-m_r)^2}{s_r^2} + \frac{(z-m_z)^2}{s_z^2}\right]\right\} \quad [14]$$

where m_r and s_r are the mean and standard deviations, respectively, of u in the radial direction, m_z and s_z are the mean and standard deviations, respectively, in the z direction, and β is a scaling parameter. The hourly transpiration rate, $T(t)$, was calculated using (Coelho and Or, 1996a)

$$T(t) = \frac{T^* \, Sin^n(\omega t)}{\int_0^{24} Sin^n(\omega t)\,dt} \quad [15]$$

where $\omega = 2\pi/P$, P is the period of the modified sine function used to approximate the hourly transpiration, n is a parameter for controlling the shape of the sine function, t is time, T^* is the total daily transpiration rate.

In the third step we calculate the resultant transient water content with the local soil volume under consideration (hence the volume balance) as:

$$\theta(r,z,t) = \theta_{flow}(r,z,t) - \Delta\theta_{uptake}(r,z,t - t_0) \quad [16]$$

Note that $\theta_{flow}(r,z,t)$ is the predicted water content obtained by the solution of Eq. [9] to [12] (using either van Genuchten [1980] or Russo [1988] retention models), that is water content due to flow from a point source only (ignoring root water uptake).

Hydrus-2D Numerical Simulation Model

In simulating soil water dynamics the H2D model numerically solves a modified form of the Richards' equation (Simunek et al., 1999)

$$\frac{\partial\theta}{\partial t} = \frac{\partial}{\partial x_i}\left[K(K_{ij}^A\frac{\partial h}{\partial x_j} + K_{iz}^A)\right] - S \quad [17]$$

where θ is the volumetric water content $[L^3\,L^{-3}]$, h is the soil water head [L], S is a sink term $[T^{-1}]$, x_i (i = 1,2) are the spatial coordinates [L], t is time [T], K_{ij}^A and K_{iz} are the components of a dimensionless anisotropy hydraulic conductivity tensor K^A, and $K(h,x,z)$ is the unsaturated hydraulic conductivity function $[L\,T^{-1}]$ given by

$$K(h,x,z) = K_s(x,z)K_r(h,x,z) \quad [18]$$

where K_r is the relative hydraulic conductivity and K_s the saturated hydraulic conductivity $[L\,T^{-1}]$. The anisotropy tensor K_{ij}^A in Eq. [17] is used to account for an anisotropic medium (Simunek et al., 1999). In the following section we highlight the main procedures used by H2D for numerically solving Eq. [17]. The intention here is to provide the main relevant procedures used by H2D to solve both the water flow equation as well as the approximation of the sink term (representing plant water uptake). Interested readers are referred to the H2D manual for more details. Before we engage in the overview of the procedures it is appropriate to first discuss the approximation of the sink term in Eq. [17].

Approximation of the Water Uptake Sink Term

The integral of the sink term representing water uptake over the entire specified rooting zone gives the actual transpiration by the crop per unit area. The total transpiration rate over a specific rooting zone volume is given as (Simunek et al., 1999)

$$T_a = \int_\Omega S\,d\Omega \quad [19]$$

where T_a is the actual transpiration rate per unit area $[L\,T^{-1}]$, Ω in this study is the entire two-dimensional root zone domain, S is the volume of water removed per volume of soil per unit time $[T^{-1}]$. The effect of water stress can be incorporated into the S term by a water stress response function $a(h,r,z)$ as

$$S(h,r,z) = a(h,r,z)S_p(h,r,z) \quad [20]$$

where $a(h,r,z)$ is the dimensionless water stress response function (see Fig. 2 for the schematic drawing of this function), According to Fig. 2 root water uptake is zero beyond the saturation point (h_o) as well as beyond some wilting point (h_3). But root water uptake linearly increases between h_o and h_1 and also decreases linearly between h_1 and h_3. Root water uptake reaches full potential between h_1 and h_2. S_p is the potential root water uptake and is given as

$$S_p = b(r,z)L_tT_P \quad [21]$$

where $b(r,z)$ is normalized water uptake distribution $[L^{-2}]$ similar to $u(r,z)$ (Eq. [14]). The function $b(r,z)$ describes the spatial variation of S_p over Ω only. L_t is the surface area associated with the transpiration process and, T_p is the potential transpiration $[L\,T^{-1}]$.

From Eq. [19] and [21] it follows that S_p and T_p are related as

$$T_p = \frac{1}{L_t}\int_\Omega S_p\,d\Omega \quad [22]$$

From Eq. [21] and [22] then the actual water uptake distribution is

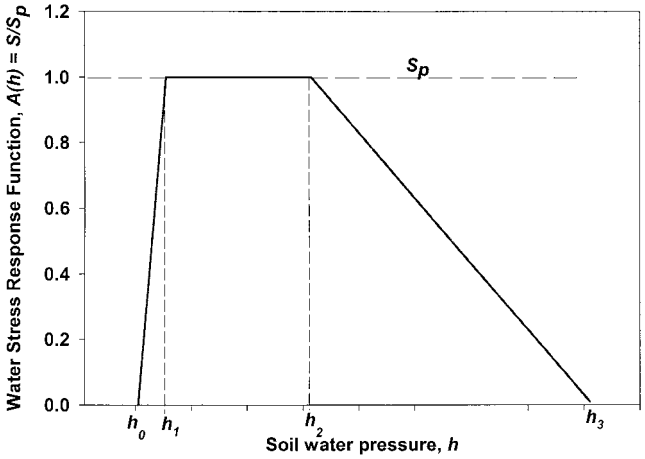

Fig. 2. Schematic shape of the root water uptake term, *S*, as function of the absolute value of the soil water head, *h*, (Source: Feddes et al., 1978; Simunek et al., 1999).

$$S(h,r,z) = a(h,r,z)b(h,r,z)L_t T_p \quad [23]$$

Then the actual transpiration rate, T_a is given by

$$T_a = \frac{1}{L_t}\int_\Omega S\mathrm{d}\Omega = T_p \int_\Omega a(h, r, z)b(r,z)\mathrm{d}\Omega \quad [24]$$

Numerical Solution of the Water Flow Equation

Hydrus-2D numerically solves Eq. [17] for variably saturated porous media using the Galerkin finite element method. The program can handle flow domains that are delineated with irregular boundaries as well as both with and without root uptake of water. The specified flow domain is divided into a network of triangular elements and the corners of these elements are taken to be the nodal points for any given flow region.

The soil water head function at a given time is approximated by (Simunek et al., 1999)

$$h(x, z, t) = \sum_{n=1}^{N} \phi_n (x, z)h_n (t) \quad [25]$$

where ϕ_n are piecewise linear basis functions satisfying the condition $\phi_n(x_m,z_m) = \delta_{nm}$, h_n are unknown coefficients representing the solution of Eq. [17] at nodal points, δ_{mn} is the Kronecker delta, N is the total number of nodal points. Following simplifying assumptions and intermediate steps, Eq. [17] leads to a system of time dependent ordinary differential equations with nonlinear coefficients in matrix form, which is then solved by an implicit finite difference scheme (Simunek et al., 1999) given by

$$[F]\frac{\{\theta\}_{j+1} - \{\theta\}_j}{\Delta t_j} + [A]_{j+1}\{h\}_{j+1} = \{Q\}_j - \{B\}_{j+1} - \{D\}_j \quad [26]$$

Where $j+1$ denotes the current time level at which the solution is being considered, j refers to the previous time level, and $\Delta t_j = t_{j+1} - t_j$, A, B, D, F, Q, and θ are coefficients and functions of h. Equation [26] is solved for specified initial and boundary conditions at given nodes within the flow domain. Details of the coefficients in Eq. [26] can be found in the H2D manual.

MATERIALS AND METHODS

Experiments

Field and greenhouse experiments were conducted in Millville(coarse-silty, carbonatic, mesic Typhic Haploxerolls) silt loam soil, with an average bulk density of 1.37 Mg m^{-3}. Details of other hydraulic properties of Millville silt loam soil have been provided by Or and Hanks (1992), Coelho and Or (1996a,b), and Or and Coelho (1996) are listed in Table 1. Experiments were conducted to determine root water uptake patterns and intensity by drip irrigated corn plants from measurements of spatial and temporal variations in θ. The experiments were performed both under cropped and non-cropped conditions within the same soil volume (Mmolawa, 2000).

Table 1. Bulk density and soil hydraulic parameters for Millville silt loam soil (Or and Hanks, 1992; Coelho and Or, 1996a, b).

Soil parameter	Value
Bulk density, Mg m^{-3}	1.37
n	1.429
α_{VG}, m^{-1}	1.622
α, m^{-1}	2.877
θ_r, m^3 m^{-3}	0.045
θ_s, m^3 m^{-3}	0.434
K_s, m h^{-1}	0.021

Pressure compensating emitters (RAAM, Netafim USA, Fresno, CA) with flow rate of 1.6 L h^{-1} were used in all experiments. (Mention of product names does not necessarily endorse these products). Irrigation was performed to meet crop water requirements based on potential evapotranspiration that was estimated from an evaporation pan in the greenhouse experiments. For the field experiments, data from the nearby meteorological weather station were used to calculate evapotranspiration and crop requirement ($ET_c = K_c\ ET_o$); where K_c is the crop cofficient and ET_o is the reference evapotranspiration calculated using the Penman-Monteith equation.

Field Experiments

Field experiments were conducted at the Utah State University Greenville Research Farm (Logan, Utah) during the summers of 1997 and 1998. Corn (*Zea mays*) was planted at 1-m row spacing with plant spacing of 0.1 m along a row. Time Domain Reflectometry (TDR) probes (three-rod design, 0.15 m long) were installed on a 0.1 by 0.1 m grid perpendicular to the crop row (see Fig. 1). There were four such monitoring grids in the field, but this paper addresses only the results obtained from an experiment with a buried dripper on crop row. Continuous and automated readings of soil water content (θ) and soil bulk electrical conductivity (EC_b) were taken at 20-min intervals at each measurement point within the field monitoring station.

Greenhouse Experiments

The same TDR configuration used for field experiments was also employed in the greenhouse experiments, using large containers (0.8 by 0.8 by 1.2 m). Emitter configurations under greenhouse experiments were limited to only subsurface and surface emitters on crop row. Corn plants were planted at 0.1-m spacing to emulate a field crop row. The soil water content monitoring interval for the greenhouse experiments was 30 min.

Hydraulic Parameter Estimation for the Analytical Model

The van Genuchten (1980) soil water characteristics parameters (Table 1) were used to obtain pressure head (h) values from measured water content. The resulting h values were used to plot unsaturated hydraulic conductivity [$K(h)$](Fig. 3a) using the relations $K(h) = K_r(h) \times K_s$, where K_r—the relative hydraulic conductivity (van Genuchten, 1980) is given by

$$K_r (h) = \frac{1 - (\alpha_{VG}h)^{n-2}\left[1 + (\alpha_{VG}h)^n\right]^{-m}}{\left[1 + (\alpha_{VG}h)^n\right]^{2m}} \quad [27]$$

The soil hydraulic parameters (α and K_s) used for linearizing the Warrick (1974) analytical solution were determined as follows: The natural logarithm of Eq. [3] was equated to the $\ln[K(h)]$ versus h (Fig. 3a), giving a tangent line $\ln K(h) = \ln(ks) + \alpha h$. The slopes of the tangent lines in Fig. 3a give the values of α and the intercepts are $\ln(K_s)$. Different intervals of h (or θ) were selected to match the measured ranges of water contents in the field. Figure 3a shows an example of three values for α and K_s for three ranges of observed h (or θ) (see Table 2). Other details on this procedure have been provided by Moldrup et al. (1989). The objective of this procedure was to obtain α and K_s values for determination of the values of k for a range of h values using Eq. [28].

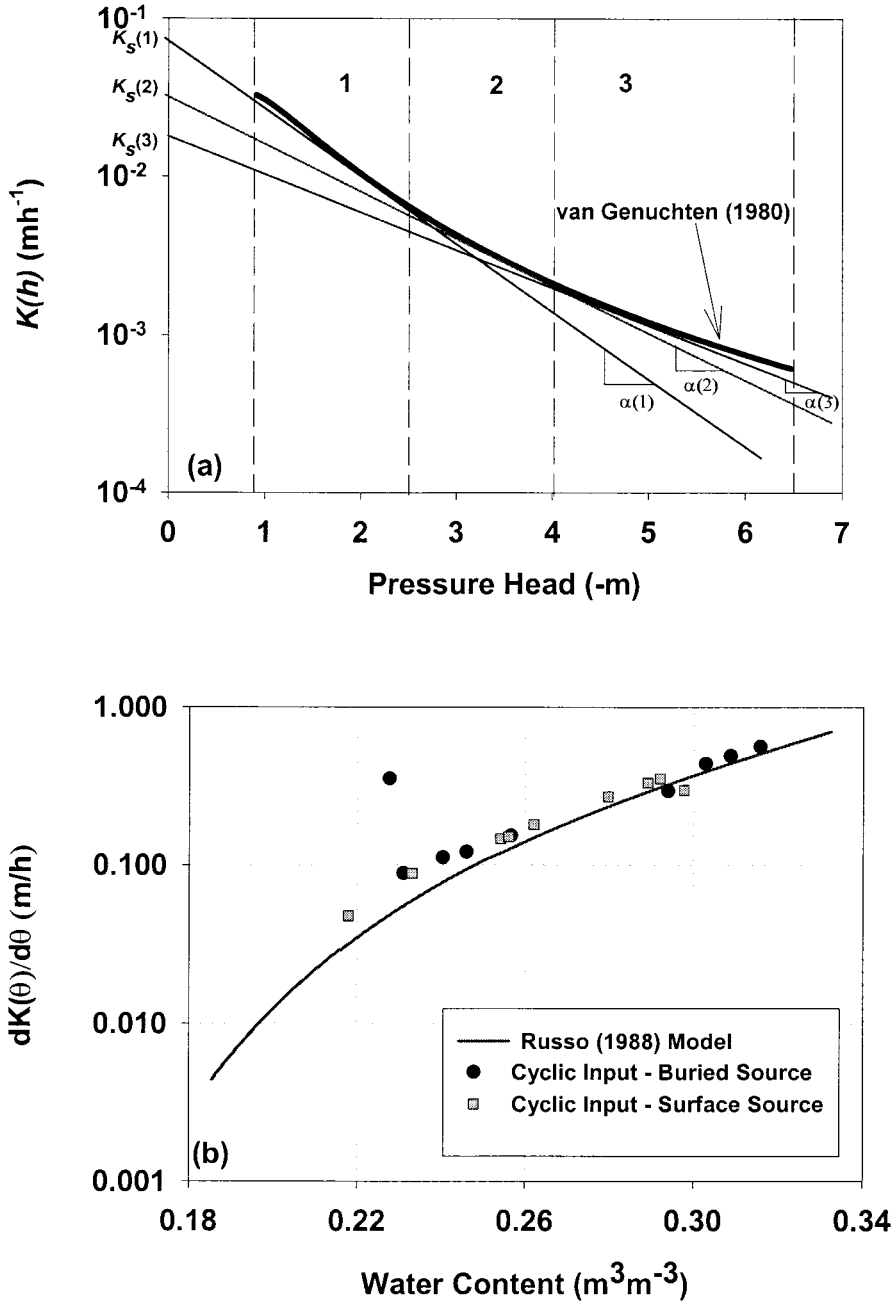

Fig. 3. Illustration of water flow parameter estimation for linearizing the Warrick (1974) analytical flow model, (a) successive approximations of α and K_s by using tangents to the $K(h)$ versus h curve, (see Table 2 for values), (b) estimated $k(\theta) = dK(\theta)/d\theta$ using the van Genuchten (1980) model and some estimated $k(\theta)$ values from flow experiments with different ranges of water content.

The additional parameter $k = dK(\theta)/d\theta$, necessary for Warrick's (1974) transient solution, was calculated for the range of water contents corresponding to the h values (Fig. 3a) using a combination of the Russo (1988) model and Eq. [3] to obtain (Or and Coelho, 1996)

Table 2. Example values for successive approximation of α, K_s, and k using the moving mean slope (see Fig. 3a).

Interval	Range of pressure head, h	α	K_s	k
	−m	m^{-1}	—— m h^{-1} ——	
1	0.91–2.5	0.9	0.07	0.56
2	2.5–4.0	0.8	0.07	0.11
3	4.0–6.5	0.7	0.06	0.01

$$k = \frac{dK(\theta)}{d\theta} = \frac{5K_s \exp(0.6h)\,[(1 - 0.5\alpha h)]^{0.2}}{(\theta_s - \theta_r)\alpha h} \quad [28]$$

where α and K_s are determined as outlined above. Equation [28] was used to plot Fig. 3b. Some k values obtained by fitting Warrick (1974) to measured θ were compared with the k function determined through Eq. [28] as shown in Fig. 3b. The fitted k values are generally higher than the k function values obtained through Eq. [28].

Estimation of the Water Uptake Function, $u^*(r,z)$, for the Analytical Model

Water uptake intensity $u(r,z)$ at a given location was estimated by normalizing the change in water content at that

soil volume by the total water content change in the entire monitoring zone for a selected time interval (e.g., 6 h). From Fig. 1b each volumetric water content change ($\Delta\theta$) monitored volume is 0.1 by 0.1 by 0.15 m. The total water content associated with the entire monitored cross-sectional volume (shown by Fig. 1a) is 1.44 $m^3\ m^{-3}d^{-1}$. For the volume elements of Fig. 1 this gives a total daily $\Delta\theta$ of 0.00216 m^3d^{-1}. This total daily uptake may be attributed to a soil surface area of 0.4 by 0.15 m = 0.06 m^2 (A_2) for consideration of transpiration within the monitored volume elements, leading to a transpiration rate of 36 mm d^{-1} (T_2). This value of transpiration rate is about five times the field averaged transpiration rate of 5 to 7 mm d^{-1} (T_1). This disparity reflects the non-uniformity of root water uptake, which is critically dependent on the distance from the dripper. It should be noted that the monitoring cross-section is centered on the dripper plane where conditions are optimal leading to a concentrated uptake at this plane. When total transpiration inferred from uptake is divided by field area associated with a single dripper the expected value of 5 to 7 mm d^{-1} is recovered. The unit field area for transpiration is the product of dripper spacing (1 m) and row spacing (1 m), with A_1 = 1 m^2. Another important aspect of the uptake function is the conversion from a cross-sectional representation to a full cylindrical coordinate system (representing the entire volume of the crop root zone). We make the assumption that the uptake pattern in the two-dimensional monitored cross-section is representative of the full three-dimensional pattern (obtained by revolution of the two-dimensional uptake pattern about the dripper axis of symmetry).

Equation [14] was fitted to the normalized water uptake intensity values and by an optimization procedure, the values β, s_r, s_z, m_z, and m_r were approximated. The fitted values for the transpiration (Eq. [15]) (also see Fig. 4) for this experimental data are such that n = 8, p = 96 h, $\omega = 2\pi/p$ = 0.065 h^{-1}, T^* is the total daily transpiration (about 5–7 mm d^{-1}). This fitted transpiration ensures that total daily transpiration is about 5 to 7 mm d^{-1}. The water uptake function, $u^*(r,z) = u(r,z) \times T$, is a product of the water uptake intensity and the transpiration rate. Detailed procedures for approximating uptake intensities have been provided by Coelho and Or, (1996a).

Water Uptake Function for Hydrus-2D

The sink term (see above *Approximation of the Water Uptake Sink Term*) required by the H2D model depends on the water uptake distribution function. We used the same fitted u-function (see Fig. 4 and Eq. [14]) used in the analytical solution to determine the water uptake distribution function for the H2D simulations. Under the H2D cylindrical coordinate system, the elemental monitoring volumes for $\Delta\theta$ (Fig. 1b) can now be transformed and represented as elemental cylinders of height, h = 0.1 m, with radii varying from 0.1 to 0.4 m from the axis of the dripper. To find the total daily water uptake (TWU) in the three-dimensional set up, the product of u and the volume (rotated volumes around the axis of the dripper) of these cylinders are summed over the simulation domain as

$$TWU = \sum_{j=0}^{n} \sum_{i=0}^{m} u(r_i, z_j) 2\pi r_i \Delta r \Delta z \qquad [29]$$

where $u(r_i,z_j)$ is the uptake intensity at a given spatial location (r,z) as given by Eq. [14], i and j are index counters, m and n are total numbers of radii and depths considered. This transformation of TWU from a two-dimensional cross-sectional representation (Fig. 4) to a three-dimensional representation (Fig. 5) is limited to cases where there is axial symmetry of u about the axis of the dripper. This usually applies only to cases where the dripper is on crop row.

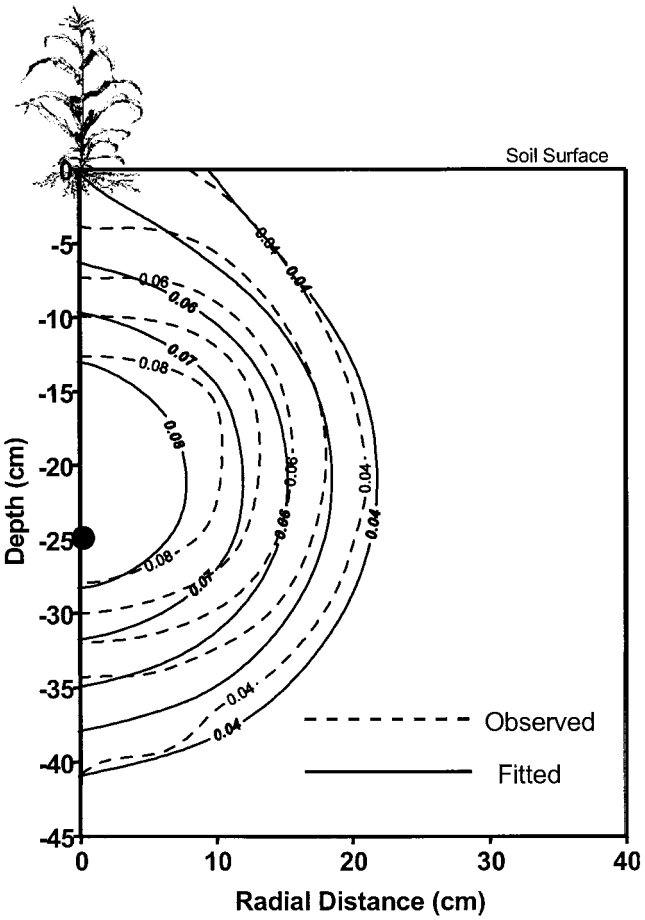

Fig. 4. Two-dimensional cross-section of the observed and fitted uptake intensity ($m^3\ m^{-3}\ d^{-1}$) distribution around a buried dripper on crop row of a field grown corn plant 83 DAE. The discharge rate of the dripper is 1.6 L h^{-1}. For these measurements the observed total daily water content change is 1.44 $m^3\ d^{-1}$.

The total daily water uptake obtained (0.057 $m^3\ d^{-1}$) through Eq. [29] is associated with an overlaying circular surface area, A_3 = 0.5 m^2, with a radius of 0.4 m. Thus TWU combined with A_3 lead to an inferred transpiration rate of 11 mm d^{-1} (T_3) This transpiration rate is about one third of the cross-sectional two-dimensional transpiration rate (36 mm d^{-1}). However, because A_3 is about one half of A_1, the resulting T_1 is expected to be one half (5.5 mm d^{-1}) of 11 mm d^{-1}, which is compatible with typical values for field averaged transpiration rate.

RESULTS AND DISCUSSION

Evaluation of Soil Hydraulic Parameters—No Plants

To use the analytical model to calculate soil water dynamics under active plant uptake, the Warrick (1974) solution in terms of the matric flux potential (ϕ) was converted to a transient θ_{flow} using Eq. [9] to [11]. The resulting theoretical θ_{flow} was then fitted to measured water content using both the van Genuchten parameters, as well as the Gardner-Warrick α, K_s and k as fitting parameters. Figure 6a shows the fitting of the theoretical θ_{flow} to measured θ for a selected point 0.1 m above a buried dripper.

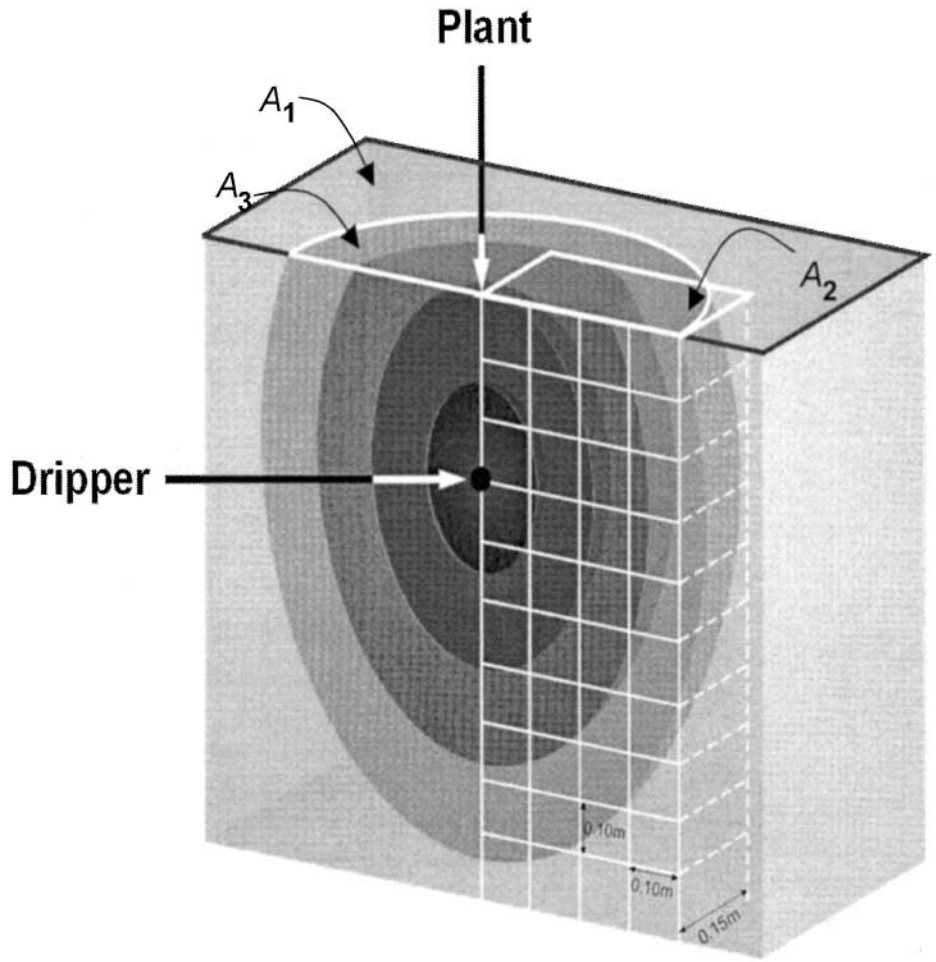

Fig. 5. Illustration of the three-dimensional water uptake transformed from the two-dimensional cross-sectional uptake, see Fig. 1a and 5. This transformed uptake pattern is attributed to a wetted circular surface area (A_3), $\pi r^2 = 0.5$ m^2, for a radius of $r = 0.40$ m. This area is one half of the total area ($A_1 = 1$ m^2) averaged transpiration area, which is a product of the emitter spacing (1 m) and row spacing (1 m). The other marked surface area $A_2 = 0.15$ m $\times$ 0.4 m $= 0.06$ m^2.

The fitted hydraulic parameters for Millville soil and the analytical model shown in Table 3 were used. The fitted VG parameters are within the range of those obtained in earlier and similar studies (Or, 1996; Coelho and Or, 1996b; Mmolawa and Or, 2000b), except that α_{vg}, α, K_s, and k are at the lower range of the typical values.

Since H2D model was used to validate the analytical model simulations, it was also calibrated for the same location ($r = 0.0$ m, z $= -0.1$ m) as the analytical model as shown by Fig. 6b. The VG water flow parameters for obtaining best fit for H2D simulations at this location are included in Table 4. These parameters are similar to those obtained by fitting the analytical model to data at the same location (see Table 1) with the exception of K_s. The value of K_s (0.025 m h^{-1}) obtained with the H2D for Millville soil was about five times larger than the K_s value (0.005 m h^{-1}) obtained by fitting the analytical model to soil water dynamics at the same location. This "anomaly" is typical to the exponential hydraulic conductivity model as discussed in a recent study by Or et al. (2000). However, the H2D K_s simulation is in agreement with typical K_s values for the Millville silt loam soil reported in other studies (Or and Hanks, 1992; Coelho and Or, 1996b).

Simulated Soil Water Dynamics at Varying Radial Distances—Without Plant Uptake

Warrick (1974) Analytical Solution Compared to Hydrus-2D Model

After evaluating both the analytical model and H2D without plants at a selected location, we then investigated the performance of both models at different radial distances from the emitter, but at a given depth relative to the point source. When the water flow parameters used by the analytical model are kept constant, and only the position (r,z) is varied, we find that the resulting water content, $\theta_{flow}(r,z,t)$, decrease as the observation point moves away from the point source. This is expected from the Warrick (1974) analytical solution subjected to the initial condition of Eq. [6]. Temporal changes in water content at a given location (r,z) tend to follow a similar pattern as simulated by the H2D for the same locations. Figure 7a shows how the analytical model soil water dynamics vary with time at increasing radial distance from the point source for a given depth (i.e., z $= -0.10$ m). When α, K_s, and k parameters estimated at a different location are used, the resulting temporal water content dynamics will be different owing

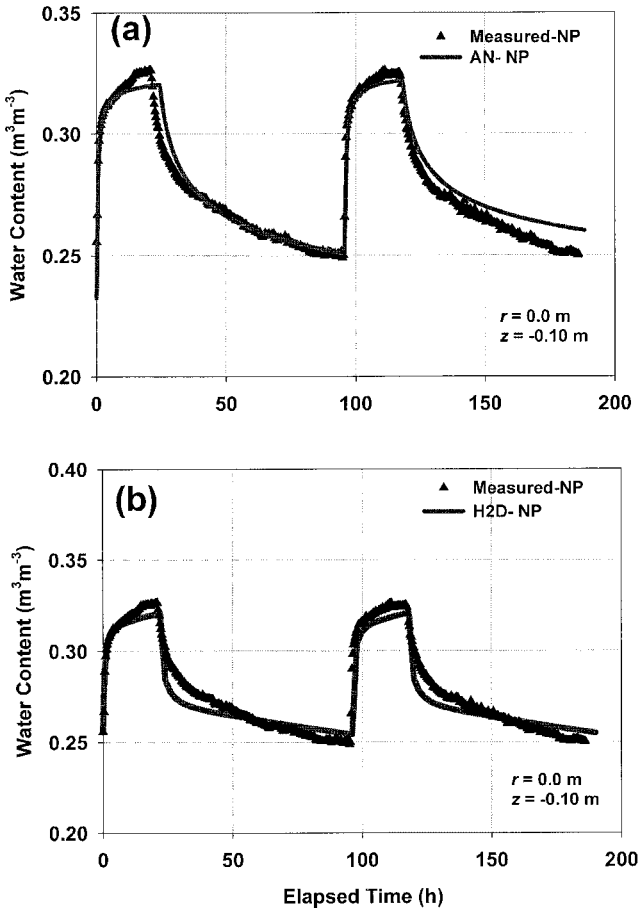

Fig. 6. Fitting of the two models to obtain water flow parameters. (a) Analytical model fitted to measured soil water dynamics without plants at a location $r = 0.0$ m, $z = -0.10$ m, (b) fitting of the Hydrus 2-D (H2D) model to measured soil water dynamics without plants at a location $r = 0.0$ m, $z = -0.10$ m.

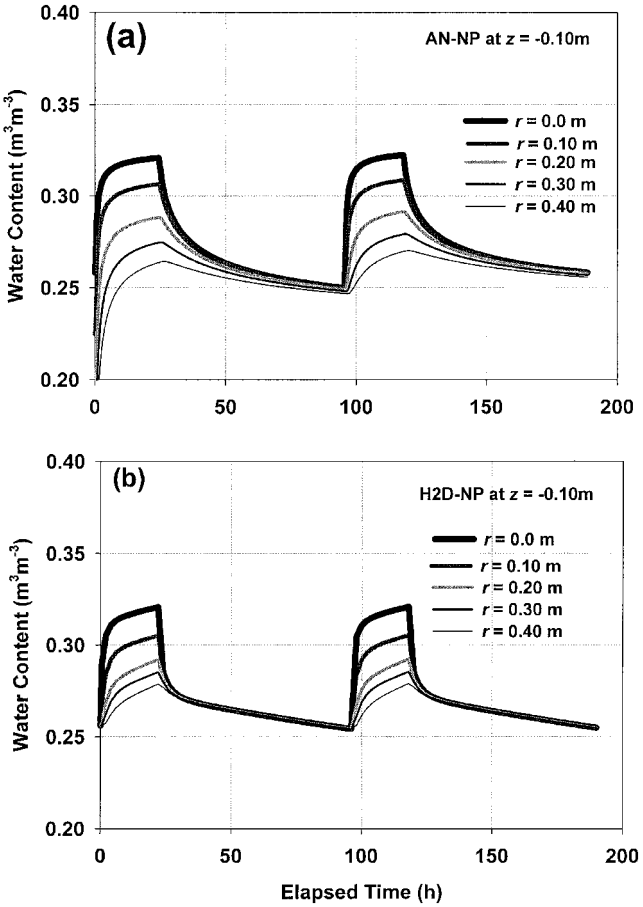

Fig. 7. (a) Observation of soil water dynamics by the analytical model simulation at a depth $z = -0.10$ m with observation points at different radial distances from the point source. (b) Observation of soil water dynamics by Hydrus 2-D (H2D) model at a depth $z = -0.10$ m with observation points at different radial distances from the point source.

to different initial water content, as well as different linearizing parameters. This is key to application of the analytical model, as a representative location and parameter set are needed.

Similar variations in water content as the observation point moves away from the point source were observed for H2D simulation as illustrated in Fig. 7b. H2D simulations show that redistribution for all the observation points attain the same water content value but with a decreasing maximum water content value with distance from the emitter. Subsequently, the initial water content for the next irrigation cycle was uniform for the H2D simulations. But the entire simulation domain for H2D had uniform initial water content. In summary, results show that the Warrick (1974) analytical solution predicts soil water dynamics similar to those simulated by H2D for different radial distances (at a fixed $z = -0.10$ m).

Table 3. Hydraulic parameters obtained after fitting the Warrick (1974) analytical solution to an observation point of time domain reflectometry (TDR) measured volumetric water content in Millville silt loam soil.†

Soil parameter	Value
α_{VG}, m^{-1}	0.133
n	1.575
θ_r, $m^3\ m^{-3}$	0.043
θ_s, $m^3\ m^{-3}$	0.463
α, m^{-1}	0.244
K_s, m h^{-1}	0.005
k, m h^{-1}	0.002

† The observation point is 0.1 m above the axis of a subsurface dripper, $r = 0.0$ m and $z = -0.1$ m. The initial water content was $\theta_i = 0.2558$ $m^3\ m^{-3}$.

Soil Water Dynamics—Considering Plant Uptake

Model Testing at a Fixed Location

The same soil hydraulic parameters used for the "no plant" scenario are used for simulation with plants. Hence,

Table 4. Water flow parameters obtained after fitting the numerical Hydrus 2D model to an observation point of time domain reflectometry (TDR) measured volumetric water content in Millville silt loam soil.†

Soil parameter	Value
α_{VG}, m^{-1}	0.160
n	1.800
θ_r, $m^3\ m^{-3}$	0.045
θ_s, $m^3\ m^{-3}$	0.45
K_s, m h^{-1}	0.025

† The observation point is 0.1 m above the axis of a subsurface dripper, $r = 0.0$ m and $z = -0.1$ m. The initial water content was $\theta_i = 0.2558$ $m^3\ m^{-3}$.

differences in soil water dynamics between the two scenarios will be attributed primarily to root water uptake. Figure 8a shows the fitting of the analytical model to measured water contents at (r = 0.0 m, z = −0.10 m). The analytical model fits measured data well except during the redistribution phase following the second irrigation. The average potential ET during the first irrigation cycle was 7.8 mm d^{-1}, and 4 mm d^{-1} during the second cycle. Variations in uptake intensity and initial water content induced by the different ET values could be the source of the poor fit by the analytical model for the second irrigation cycle, despite using the correct potential ET values.

As Fig. 8b depicts, H2D model better captures the soil water dynamics at the selected location than the analytical model especially during the second redistribution phase. This is likely to be due the fact that the H2D model water extraction function incorporates both the climatic conditions as well as the soil water status. Whereas the analytical model water uptake function only considers the climatic conditions and not soil water status (see *Comparison of models and data at arbitrary locations* below for more explanation).

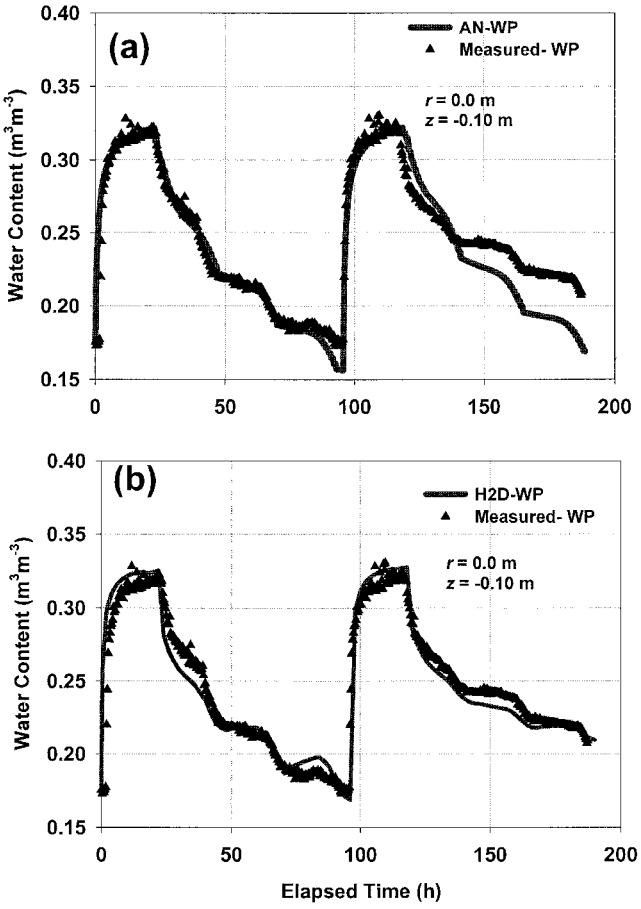

Fig. 8. Fitting of the analytical and Hydrus 2-D(H2D) models to measured data at r = 0.10 m, z = −0.10 m in presence of plants. (a) Analytical model fitted to measured soil water dynamics with plants at a location r = 0.0 m, z = −0.10 m, (b) H2D model fitting to measured soil water dynamics with plants at a location r = 0.0 m, z = −0.10 m.

Model Testing at Different Radial Distances

Soil water dynamics of both models in presence of active plant uptake were compared at different radial distances from the point source so as to test the spatial performance of the analytical model with constant linearizing parameters. Figure 9a shows the temporal variations in water content with the analytical model at the same locations used in Fig. 7a. The analytical model shows a clear trend where water uptake patterns decrease with increasing distance from the source. But it can also be seen that there is pronounced cumulative water uptake for locations within 0.1 m of the location (r = 0.0 m, z = −0.10 m) where the linearizing parameters were obtained. This possibly reflects the range of applicability of the linearizing parameters and beyond a radial distance of 0.1 m different parameters may be required.

However, the H2D model shows water uptake patterns (Fig. 9b) that decrease with increasing radial distance from the point source but not as pronounced as the case with the analytical model. This is because the H2D model uses only one set of hydraulic parameters and takes into account spatial interpolation of water content and water uptake spatial patterns.

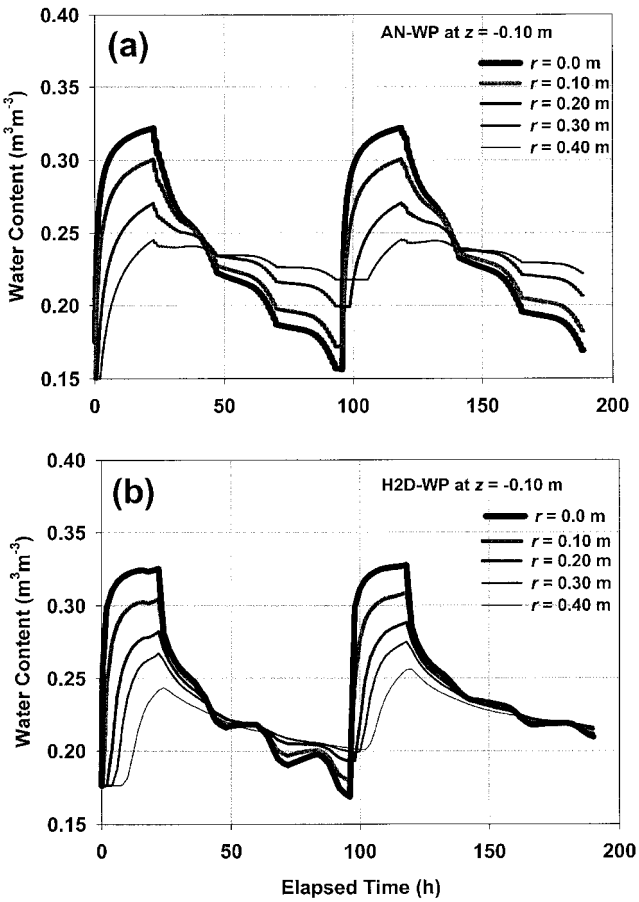

Fig. 9. Observation of soil water dynamics in presence of plants as the observation points shift radially away from the source at depth z = −0.10 m. The observation points vary from r = 0.10 m to r = 0.40 m at the same depth z = −0.10 m. (a) analytical model, (b) Hydrus 2-D (H2D) model.

Comparison of Models and Data at Arbitrary Locations

After having anchored both the H2D and the analytical models and compared them at different observation points from the dripper, two locations with soil water content measurements were chosen arbitrarily, one at the dripper location (r = 0.0 m, z = 0.0 m) and another one at r = 0.20 m and z = 0.20 m. Figures 10 and 11 show a comparison of simulations by the two models with measurements at these two locations respectively. It can be seen from Fig. 10a that the analytical and H2D models redistribute water similarly although they do not reach the same maximum values of water content. The analytical model matches the measured saturation at this location, but it starts at higher water content than that measured. When water uptake by plant roots was considered at this location (Fig. 10b), both methods overestimated the water uptake by plants as compared with measured data. Qualitatively, H2D was in a better agreement with measurements than the analytical model.

When the two models are compared at r = 0.20 m, z = 0.20 m location (Fig. 11), they both closely match measured data during the redistribution phase in the absence of plants (more so than during the irrigation phase). Figure 11a also shows that the H2D and analytical models closely matching each other at this location. As was the case with the observation point close to the dripper, comparisons of these models in the presence of plants at r = 0.20 m, z = 0.20 m show the analytical model overestimating the root water uptake and H2D doing a better job matching the measured data (see Fig. 11b). Both models have lower starting water content values than the measured water content and therefore redistribution is bound to be different especially when plants are present.

From these model comparisons with measured data (Fig. 10 and 11), both models perform relatively better in predicting soil water dynamics in the absence of plants than when plants were present, especially during the redistribution phases. However when plants are considered the analytical model tends to overestimate root water uptake as compared with H2D. This can be explained by the fact that with the H2D model the water uptake function determined through a sink term (S) that incorporates a water stress response function which regulates the water uptake rates (see Fig. 2 and Eq. [21]). This function ensures that root water uptake is only calculated at specified water content or h ranges. For example Fig. 2, considering absolute values of h,

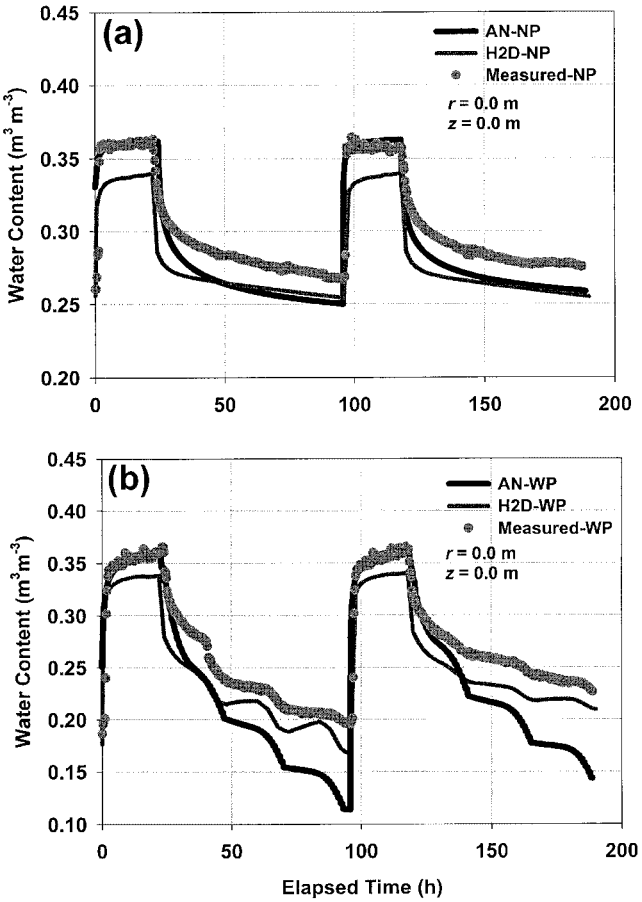

Fig. 10. Temporal soil water dynamics comparison of measured water content data at r = 0.0 m, z = 0.0 m to the two models (a) in the absence of root water uptake, (b) in the presence of root water uptake.

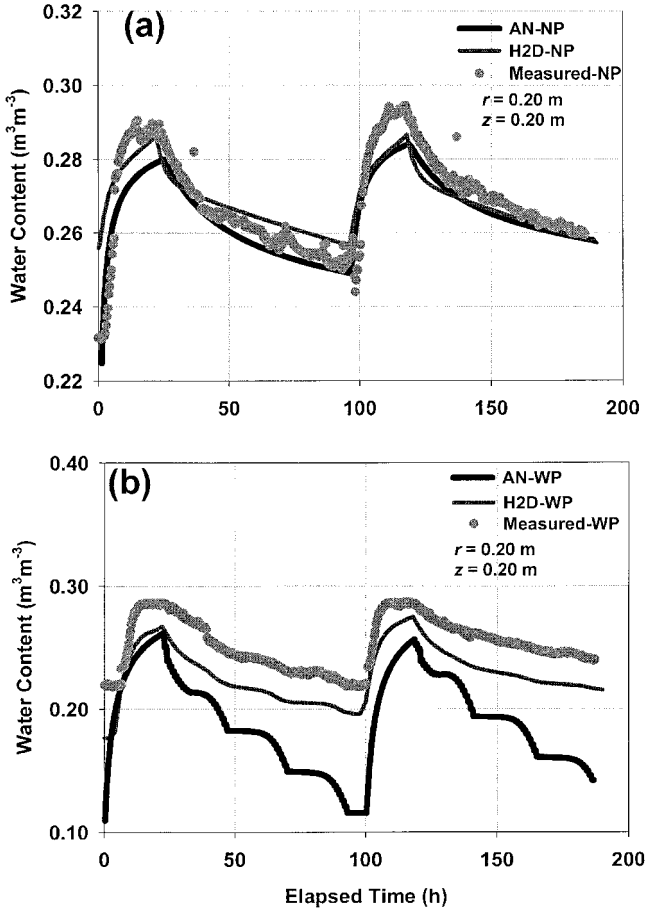

Fig. 11. Depicts the comparison of soil water dynamics with and without plants between Hydrus 2-D (H2D) and the analytical model at a monitored location r = 0.20 m, z = 0.20 m, (a) without plants and (b) with plants.

plants will keep taking up water from h_0 to h_1 in an increasing manner reaching a plateau between h_1 and h_2. From h_2 to h_3 plant uptake of water is at a decreasing rate and will cease beyond h_3 where plants wilt. This water stress response function more realistically reflects the plant water uptake mechanism. However, the analytical model does not incorporate any water stress response function to cater to changing water uptake patterns in response to the changing water status of the soil-water-plant continuum. Thus the analytical model assumes constant root water extraction regardless of the changing soil water status. Therefore the analytical model runs the risk of overestimating actual root water uptake by plants.

Another aspect of the analytical model is that the linearizing parameters are not constant throughout the entire soil profile. They are water content dependent (see Fig. 3) and therefore different locations have different water content values and are likely to be governed by different values of linearizing parameters.

Comparisons for an Entire Root-Zone Cross-Section

Water Flow—No Plants

A comparison of the two models was extended to the two-dimensional monitored cross-section. This was done to further evaluate the performance of the analytical model using a single set of linearizing hydraulic parameters over the entire monitored cross-section. Figure 12 shows a snapshot of the water content distribution during irrigation (at t = 10 h). The results illustrate how the models compare with measured water content values (with symbols) during irrigation in the absence of plants.

Figure 12 shows that H2D (Fig. 12b) reaches a slightly lower values of water content distribution around the point source, but generally matches the measured water content profile better than the analytical model (Fig. 12a) especially for locations at $r > 10$ cm. On the other hand the analytical model matches the measured data points around or close to the dripper ($r < 10$ cm) better than the H2D but somewhat poorly for locations at radial distances >10 cm. The analytical model depicts wetter conditions closer to the dripper and less wetting at points away from the point source.

Water Flow with Plant Water Uptake

Soil water dynamics simulated by the two models were compared during the irrigation phase and a short time before the next irrigation cycle when plant water uptake has been taking place (and modifying water distribution). Figures 13 and 14 illustrate comparisons of measured soil water distribution with simulations by both models for 10 h during irrigation and 5 h before the onset of another irrigation cycle, respectively. Figure 13a shows that the analytical model matches the measured data closely in the area around the dripper and underestimates the water distribution further away from the point source. Hydrus-2D on the other hand better estimates the water distribution over the entire cross-section than the analytical model does.

Figure 14 depicts measured soil water distributions and simulations by the two models 5 h before the onset of the next irrigation cycle, (4-d cycle in this case). The analytical model shows higher plant uptake around the dripper (Fig. 14a). The analytically predicted water content distribution around the dripper reaches 0.10 $m^3\ m^{-3}$ whereas the measured data and H2D (Fig. 14b) show an average water content distribution of about 0.19 $m^3\ m^{-3}$. For the rest of the monitored cross-sectional water content Fig. 14 shows values close to 0.20 $m^3\ m^{-3}$ except for the top layer (5–10 cm below the surface). It is interesting that the H2D model shows water content distribution in the range of 0.19 to 0.20 $m^3\ m^{-3}$ for the

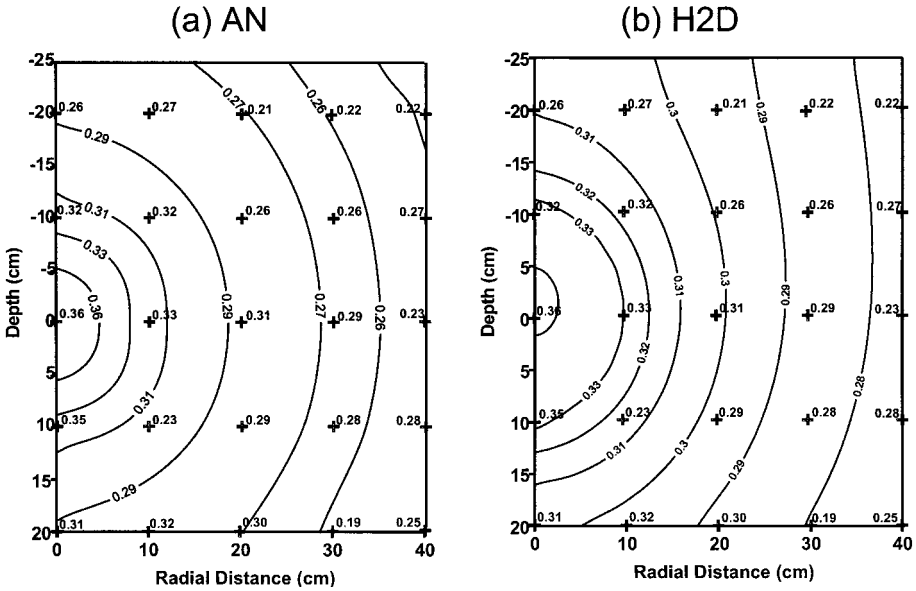

Fig. 12. Illustration of soil water distribution both measured and predicted in absence of plants in a two-dimensional space at t = 10 h since the start of irrigation. For (a) analytical model and (b) H2D model.

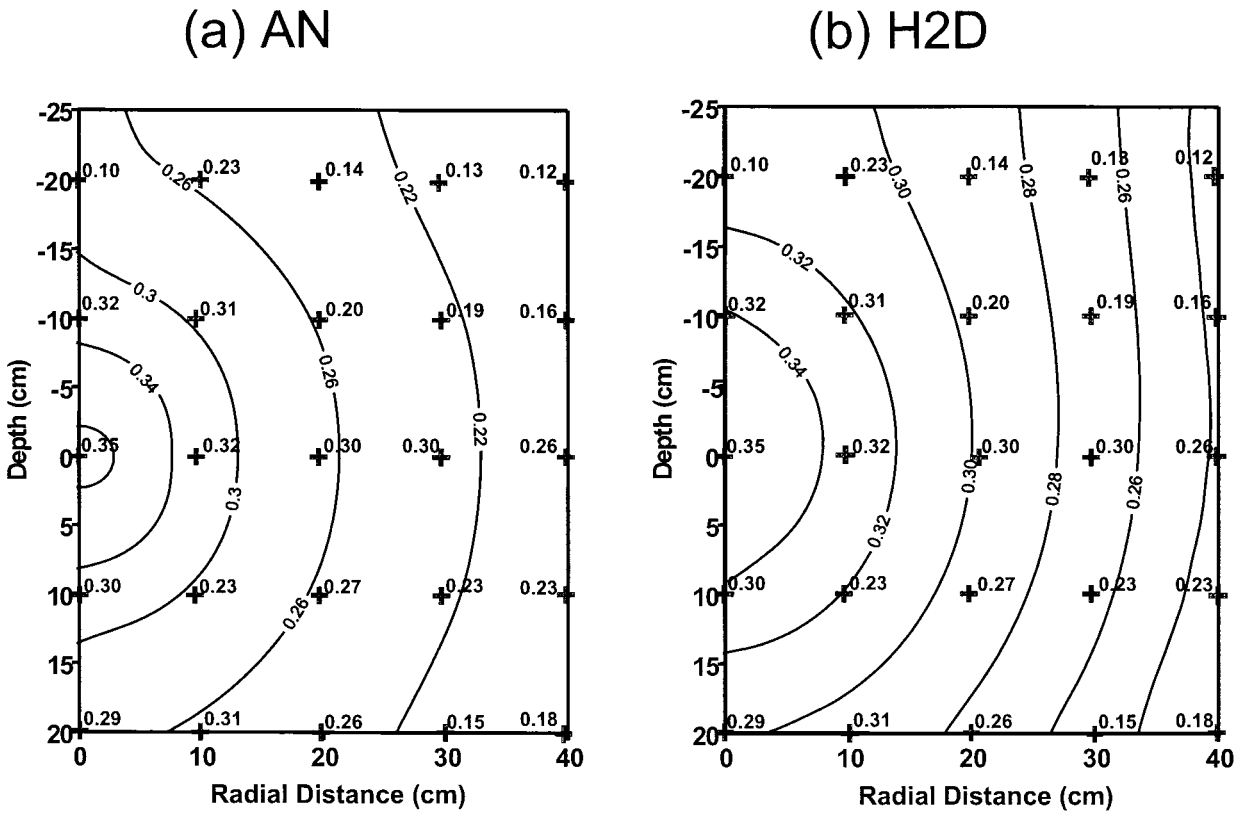

Fig. 13. Comparison of measured and predicted soil water dynamics in the presence of plants in 2D space at t = 10 h since the start of irrigation. The irrigation interval is 4 d. (a) Comparison of the analytical model simulation to measured data, (b) H2D compared with measured data.

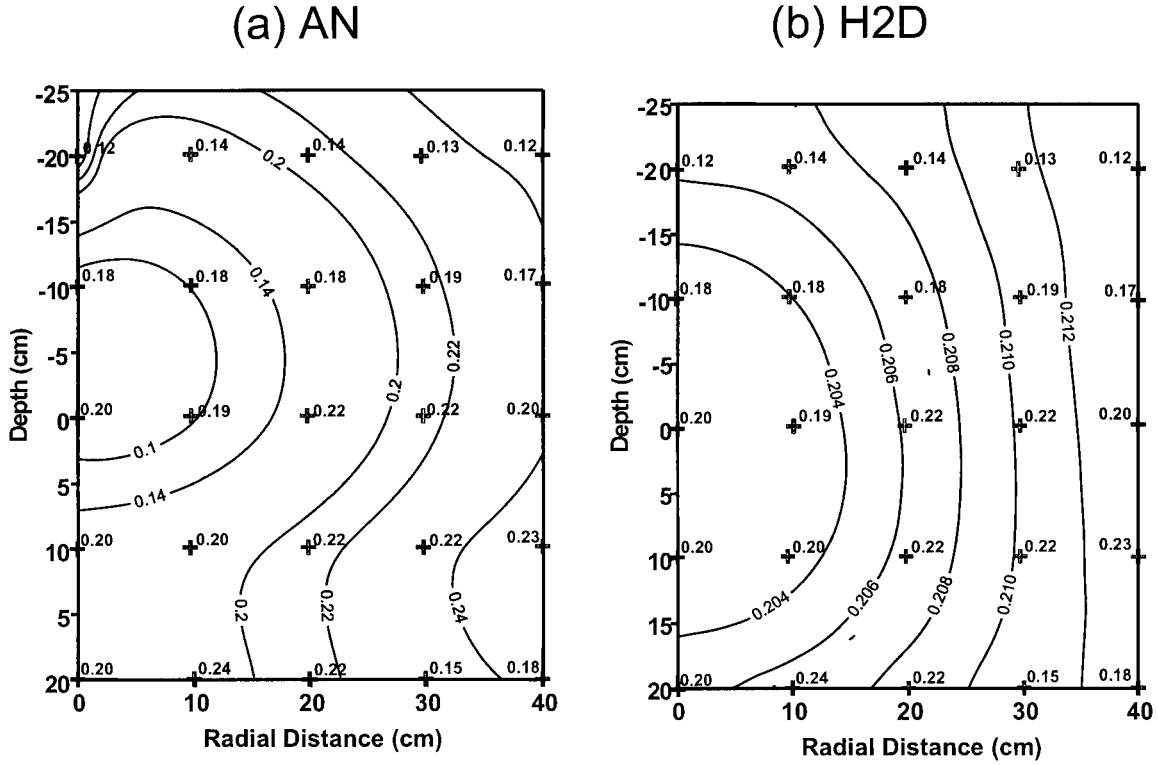

Fig. 14. Comparison of measured and predicted soil water dynamics in the presence of plants in two-dimensional space at 5 h before the onset of irrigation (the irrigation interval is 4 d). Comparison of (a) the analytical model simulation and (b)Hydrus 2-D (H2D) compared with measured data.

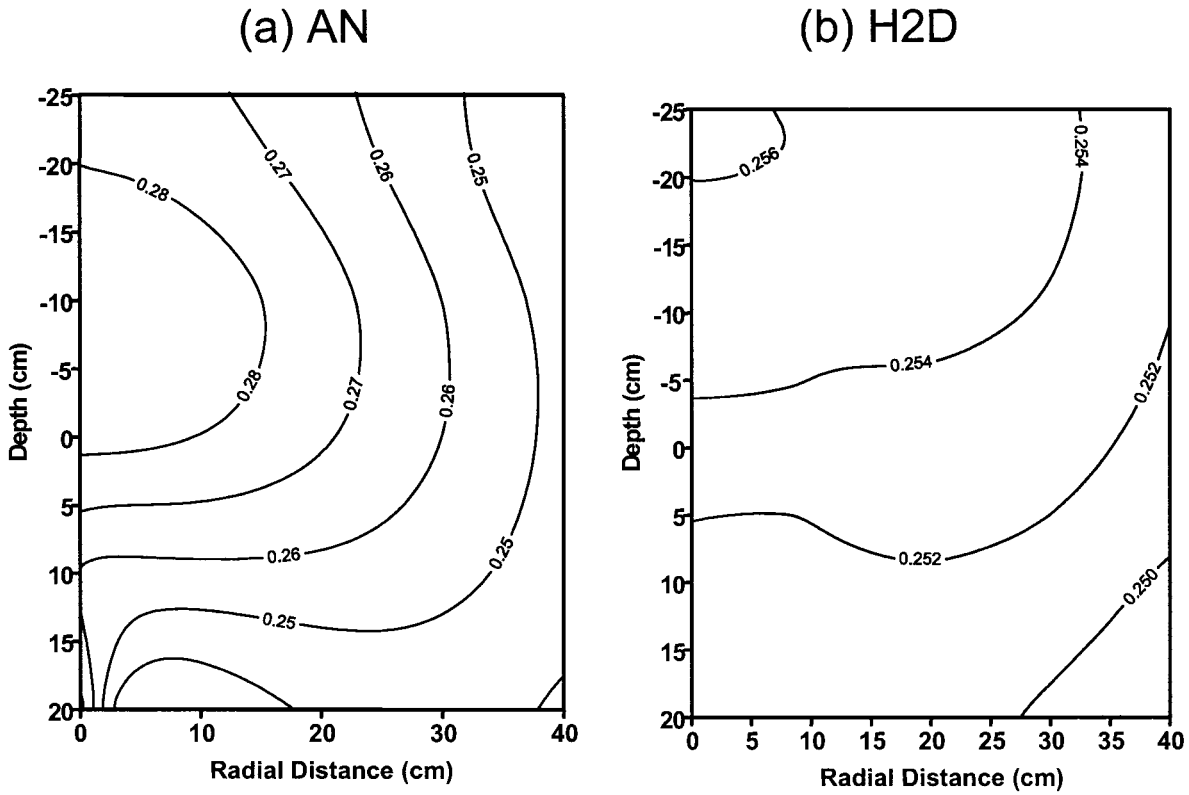

Fig. 15. Simulated soil water dynamics in the presence of plants in a two-dimensional space at 5 h before the start of irrigation (the irrigation interval is 1 d). Comparison of (a) the analytical model and (b) Hydrus 2-D (H2D) model.

entire cross-section (Fig. 14b), whereas the analytical model (Fig. 14a) shows varying water content from 0.10 to 0.24 $m^3\ m^{-3}$ over the same domain.

Figures 13 and 14 show soil water dynamics for a 4-d irrigation interval. In addition, we investigated the effect of longer irrigation time relative to a shorter water uptake opportunity time by altering the irrigation interval to one day. In contrast with the 4-d irrigation interval where root water uptake period is much larger than water application time, for the 1-d irrigation interval water flow time is similar to plant water uptake time scale.

Figure 15 depicts water content distribution 5 h before the onset of the next irrigation for a 1-d irrigation interval simulated by the two models. It can be seen from Fig. 15a that water content is higher around the dripper and decreases at larger distances away from the dripper. This is in sharp contrast to Fig. 14a (4-d irrigation interval) where there is the lowest water content around the dripper and increasing water content as we move away from the dripper. The results suggest that for longer irrigation intervals, that is, when the water uptake time is greater than the irrigation time, the superpositioning of θ_{flow} and $\Delta\theta_{uptake}$ to predict water content in the entire cross-section produces satisfactory results as shown by Fig. 14a. When flow time is longer than uptake time it is likely to expect higher water contents in the simulated cross-section. This explains why water content increases as we move away from the area around the point source. However, the area around the dripper becomes drier as compared with the entire cross-section because (i) the analytical model was anchored around this area and, (ii) the water uptake function is unbounded by soil water status. For short-irrigation intervals (1 d), that is, when water uptake time is less than the irrigation time then the superpositioning θ_{flow} and $\Delta\theta_{uptake}$ to predict water content in the entire cross-section also shows satisfactory results as shown by Fig. 15a. Since the irrigation time is longer than uptake time we are also likely to have more volumetric water content in the cross-section as there is little time for water uptake as Fig. 15a shows.

With the H2D model (Fig. 15b), water content distribution for the 1-d irrigation interval is around 0.25 $m^3\ m^{-3}$ but for the longer irrigation interval (4 d) the water content in the cross-section varies from 0.20 to 0.21 $m^3\ m^{-3}$ (see Fig. 14b). These H2D results suggest that if the plant water uptake time is shorter than the irrigation time then the water content in the 2D cross-section remains higher than the water content at which plants begin to extract some water. Consequently we are only observing moisture content redistribution just 5 h before the onset of the next irrigation (Fig. 15b).

SUMMARY AND CONCLUSIONS

Comparisons of soil water dynamics modeling both in the presence and absence of plants were made between the numerical H2D model and the analytical model that uses a local volume balance for modeling soil water dynamics. The analytical model compared fairly well with the numerical H2D model, especially for point locations at the depth ($z = -0.10$ m) where it was initialized for parameter estimation. It is apparent

from these comparisons that the analytical model is sensitive to the choice of linearizing parameters, α, K_s, and k, both in the presence and absence of plants. The water extraction function for the analytical model is insensitive to plant water stress and changing soil water content. However the water function for this model does take into consideration the climatic conditions through the incorporation of the transpiration rate. The H2D model on the other hand has a water stress function included in its water extraction function. The analytical model performs consistently similar to the H2D model for shorter and longer irrigation intervals and water uptake opportunity times. Thus the analytical model can be a useful tool for drip irrigation designers and managers because it can help predict the movement and distribution of water in crop rooting zones.

In conclusion, (i) different linearizing parameters are needed for different ranges of water contents for the analytical model to perform satisfactorily over an entire cross-section simulation; (ii) superpositioning the water uptake function with water content (without plants) is not affected by the duration of irrigation water flow nor by the water uptake time; (iii) water uptake function by the analytical model does not consider changing soil water content status and therefore tends to overestimate water uptake by plants; (iv) the H2D model generally evaluates the measured soil water dynamics in absence and presence of plant uptake more closely than the analytical model.

ACKNOWLEDGMENTS

The authors thank Markus Tuller and Scott Jones (USU) for their comments on the earlier versions of this manuscript. We are also grateful to the support of U.S.–Israel Binational Agricultural Research and Development fund (BARD). The partial support of Utah Agricultural Experimental Station (UAES) is gratefully acknowledged. Approved as UAES journal paper 7333.

REFERENCES

Aura, E. 1996. Modeling non-uniform soil water uptake by a single plant root. Plant Soil 186:237–243.

Clothier, B.E., K.R.J. Smetten, and P. Raharjo. 1990. Sprinkler irrigation, roots and uptake of water p. 101–108. Workshop on field scale water and solute flux in soils. Birkhauser Verlag, Switzerland.

Coelho, F.E., and D. Or. 1996a. A parametric model for two-dimensional water uptake intensity. Soil Sci. Soc. Am. J. 60:1039–1049.

Coelho, E.F., and D. Or. 1996b. Flow and uptake patterns affecting soil water sensor placement for drip irrigation management. Trans. ASAE 39:2007–2016.

Coelho, E.F., and D. Or. 1999. Root distribution and water uptake patterns of corn under surface and subsurface drip irrigation. Plant Soil 206:123–136.

Feddes, R.A., E. Bresler, and S.P. Neuman. 1974. Field test of a modified numerical model for water uptake by root systems. Water Resour. Res. 10:1199–1206.

Feddes, R.A., P.J. Kowalik, and H. Zaradny. 1978. Simulation of field water use and crop yield. John Wiley and Sons, New York.

Gardner, W.R. 1958. Some steady-state solutions of the unsaturated moisture flow equation with application to evaporation from water table. Soil Sci. 85:228–232.

Heinen, M. 1997. Dynamics of water and nutrients in closed, recirculating cropping systems in glasshouse horticulture: with special attention to lettuce grown in irrigated sand beds. Wageningen Agricultural University, Wageningen, Haren.

Hillel, D., H. Talpaz, and H. Van Keulen. 1976a. A macroscopic-scale model of water uptake by nonuniform root System and of water and salt movement in the soil profile. Soil Science 121:242–255.

Hillel, D., C.G.E.M. van Beek, and H. Talpaz. 1976b. A microscopic-scale model of soil water uptake and salt movement to plant roots. Soil Science 120:385–399.

Mmolawa, K.B., and D. Or. 2000a. Root zone solute dynamics under drip irrigation: A review. Plant Soil 222:163–190.

Mmolawa, K.B., and D. Or. 2000b. Water and solute dynamics under a drip irrigated crop: Experiments and analytical model. Trans. ASAE 43:1597–1608.

Mmolawa, K.B. 2000. Water and solute dynamics in drip irrigated fields. PhD Dissertation. Utah State University, Logan, UT.

Moldrup, P., D.E. Rolston, and J.A. Hansen. 1989. Rapid and numerically stable simulation of one dimensional, transient water flow in unsaturated layered soils. Soil Sci. 148:219–226.

Molz, F.J. 1971. Interaction of water uptake and root distribution. Agron. J. 63:608–610.

Or, D., and R.J. Hanks. 1992. Soil water and crop yield spatial variability induced by irrigation nonuniformity. Soil Sci. Soc. Am. J. 56:226–233.

Or, D. 1996. Drip irrigation in heterogeneous soils: Steady-state field experiments for stochastic model evaluation. Soil Sci. Soc. Am. J. 60:1339–1349.

Or, D., and F.E. Coelho. 1996. Soil water dynamics under drip irrigation: Transient flow and uptake models. Trans. ASAE 39:2017–2025.

Or, D., U. Shani, and A.W. Warrick. 2000. Subsurface tension permeametry. Water Resour. Res. 36:2043–2053.

Philip, J.R. 1971. Steady infiltration from buried, surface, and perched point and line sources in heterogeneous soils: I. Analysis. Soil Sci. Soc. Am. Proc. 36:268–273.

Russo, D. 1988. Determining soil hydraulic properties by parameter estimation: On the selection of a model for hydraulic properties. Water Resour. Res. 24:453–459.

Simunek, J., M. Sejna, and M.Th. van Genuchten. 1999. The hydrus-2D software package for simulating the two-dimensional movement of water, heat, and multiple solutes in variably saturated media. IGWC, Riverside, CA.

Spiegel, M.R., and J. Liu. 1999. Mathematical handbook of formulas and tables. McGraw-Hill, New York.

Van Genuchten, M.T. 1980. A closed-form equation for the prediction of the hydraulic conductivity of unsaturated soils. Soil Sci. Soc. Am. J. 44:892–898.

Warrick, A.W. 1974. Time-dependent linearized infiltration. I. Point sources. Soil Sci. Soc. Am. Proc. 38:383–386.